Energy partitioning in ^1S-wave electron-impact ionization of atomic hydrogen

Robin Shakeshaft*

Physics Department, University of Southern California, Los Angeles, California 90089-0484, USA

(Received 4 December 2009; published 23 March 2010)

Results of calculations of the integrated cross section and the energy distribution for ionization of ground-state hydrogen by ^1S-wave electron impact are presented. The breakup amplitude is expressed as a volume integral that contains an approximate final-state wave function which accounts for postcollision dynamic screening. The error in this wave function is accounted for by the response function, which is represented on a real discrete (Sturmian) basis, with its physical branch specified by the arrow of time. It is found that the energy distribution is primarily convex for impact energies from about 2 to 10 eV above threshold, and primarily flat from about 10 to 20 eV above threshold. The shape of the energy distribution appears to reflect both the competition between escape and recapture, and the substantial postcollision exchange of energy between the electrons. A rough, *nonclassical* criterion for predicting the curvature of the energy distribution is derived.

DOI: 10.1103/PhysRevA.81.032705 PACS number(s): 03.65.Nk

I. INTRODUCTION

Dynamical screening is believed to play an important role in electron-impact ionization of an atom [1]. The slowest electron that emerges from the collision vacillates between escape and recapture as it moves away from the nucleus. The earliest calculation of energy partitioning in two-electron escape was performed by Vinkalns and Gailitis [2] In their calculation, they followed the classical trajectories, and they found that for impact energies close to threshold, energy partitioning is uniform; i.e. the shape of the energy distribution is flat. Subsequently Read performed a more accurate, classical calculation and found that the shape of the energy distribution is convex, at least within a few eV of threshold [3,4]. He determined the deviation from uniformity to be about 6%, a result later confirmed by Gailitis [5]. However, the curvature of the energy distribution has remained a subject of debate, and results of more recent calculations have not produced a consistent picture. Rost, who used a semiclassical approach, did obtain results in accord with those of Read and Gailitis, and found the energy distribution to be convex up to about 4 eV above threshold for electron-impact ionization of hydrogen [6]. On the other hand, Bartlett and Stelbovics, who used a fully quantal approach, found the energy distribution for the same process to be concave above about 1 eV, roughly flat at 1eV, and mildly convex (a deviation from uniformity of at most 4%) below 1 eV [7]. Baertschy *et al.*, who also used a fully quantal approach but did not explore the region below 4 eV, also found the energy distribution to be concave at 4 eV and above [8].

Reid has stressed that as the electrons escape, they continue to exchange appreciable energy over a very large distance. He found that it was necessary to integrate the classical equations out to an enormous distance, thousands of Bohr radii within a few eV of threshold, to obtain convergence of the energy distribution [9]. A similar obligation was confronted by Rost, who, in his semiclassical calculations, found it necessary to integrate to 10^8 Bohr radii in the region of highly unequal energy sharing. Furthermore, Popov and Benayoun have shown that the angular distribution is strongly influenced by the long-range Coulomb torque that one electron exerts on the other [10]. In fact, unless the electrons escape in opposite directions, they each acquire angular momentum which grows logarithmically with distance, without limit [11]. The question naturally arises as to whether the concave curvature found in previous quantal calculations can be attributed to terminating the integration at an insufficiently large distance. Of course, it would be difficult to answer this question given the very slow convergence of the energy distribution with distance observed in the classical and semiclassical calculations.

The purpose of this paper is to report on theoretical results for electron-impact ionization of hydrogen obtained using an approach in which the final-state motion is partially built into the calculation. The method, described in an earlier paper, is fully quantal and is based on exploiting the analytic properties of the resolvent with respect to its underlying time scale [12]. The investigation is limited (by modest computational resources) to impact energies of 2 eV or more above threshold. It is found that for impact energies from 2 to about 10 eV above threshold, the energy distribution is primarily convex, and that it is primarily flat from roughly 10 to 20 eV above threshold. This conflicts with the results of previous quantal calculations [7,8]. It is also in sharp contrast to the results of semiclassical calculations at energies from 4 to 20 eV above threshold [6]. However, the present results are consistent with those for another elementary three-body breakup process: the double ionization of helium by one-photon impact. Quantal calculations for that process indicate that the electron energy distribution following double photoionization is either convex or flat for photon impact energies over the same range, i.e., from about 2 to 20 eV above threshold [13,14].

Furthermore, the present results are in accord with a simple, rough, *nonclassical* criterion developed in Sec. III below, namely, that the energy distribution is roughly flat in the region where the final kinetic energies E_1 and E_2 of the slow and fast electrons, respectively, satisfy

$$E_1/E_2 \gtrsim \sqrt{E_2/(1\ \mathrm{Ry})}. \tag{1}$$

Putting $E_1 = E_2 = E/2$, we infer from this criterion that at least part of the energy distribution is flat (the vicinity of equal-energy sharing) when the excess energy E is less than about

*robins@usc.edu

2 Ry. Note that quantal calculations for double photoionization of helium within 2 eV threshold were carried out by Bouri *et al.* [15]; they found that while the energy distribution does have convex structure in the region $E_1/E_2 \approx 1$, it also has a pronounced concave structure in the region $E_1/E_2 \ll 1$, a result that is consistent with the preceding criterion.

Electron-impact ionization poses a greater challenge for a theorist than does photon-impact ionization. There are at least three reasons for this; I comment on two of them now, and postpone discussion of the third to a few paragraphs hence:

(i) Electrons, in most atomic processes, typically remain far apart due to their mutual repulsion. Consequently, the singularity of the Coulomb potential at the point of confluence of the two electrons, and the associated cusp of the wave function, play only a secondary role. However, in the entrance channel for electron-impact ionization of hydrogen, the two electrons are uncorrelated. Therefore the initial unperturbed wave function is not attenuated in the spatial region where the two electrons are close, and the electron-electron singularity can affect the accuracy of a theoretical estimate of the first-order ionization amplitude. Furthermore, since this singularity plays only a secondary role in the exact wave function, its spurious influence must be canceled by the correction to the unperturbed wave function. In contrast, the electrons are strongly correlated in the ground state of helium. Hence the probability for them to be near one another in the entrance channel for photon impact ionization of helium is small, and the electron-electron singularity hardly affects the estimation of the first-order amplitude for double photoionization of helium.

(ii) Ionization of a hydrogen atom by electron impact at a few eV and more above threshold occurs through a hard collision between the electrons, so there is a significant probability for the two electrons to exchange appreciable angular momentum even before they move apart. By contrast, in double ionization of a helium atom by photon impact at a few eV and more above threshold, the photon is most likely to transfer its (unit) angular momentum to one of the electrons, while the other electron undergoes a soft collision (shakeoff); the electrons do not begin to exchange angular momentum until they are relatively far apart, when their interaction is relatively weak.

As indicated above, to obtain a converged energy distribution without integrating out to very large distances, we need to build in some information about the final state. However, the exact asymptotic form of the wave function for three charged particles at large separations [16] is not easy to implement numerically. Fortunately, many years ago Peterkop [17,18] and, independently, Rudge and Seaton [19,20] pointed out that dynamical screening in the final state can be simulated by velocity-dependent effective charges. Thus a simple approximate wave function can be constructed; let us call it the 2C wave function, since it is the product of two one-electron Coulomb wave functions. The 2C wave function describes each electron moving quasi-independently in a pure Coulomb potential whose strength is dynamic [21]. Rudge and Seaton showed that (i) the ionization amplitude can be expressed as an integral over a hypersurface of asymptotically large radius, (ii) in principle, this integral can be evaluated exactly by using the method of stationary phase, and (iii) at the point of stationary phase, the exact asymptotic wave function can be replaced without error by the 2C-wave function [22]. However, this potentially very useful result is numerically intractable because the 2C wave function is inapplicable outside the immediate vicinity of the point of stationary phase; to evaluate the surface integral, it would be necessary to average over hyperangles in the neighborhood of the point of stationary phase, a daunting task.

I have described a practical method for converting the surface-integral representation of the breakup amplitude to a volume integral [12]. The 2C wave function can be introduced into the volume integral without error. In place of the exact wave function, the volume integral calls for the exact Green's function or, rather, the exact response function which describes the scattered outgoing wave. This may seem like an expensive trade, but in fact it is not; the response function is needed only over a finite region since the volume integral is insensitive to the region of asymptotically large distances. Hence the response function can be represented on a finite discrete basis, even though the electrons may exchange energy over a distance that is larger than the characteristic range of the basis. (Of course, the larger the reaction volume in which breakup occurs, the larger must be the basis.) A similar device was applied more than 15 years ago to one-photon double ionization of helium, a process that can be viewed as a "half" collision [13]. The reason it has not been applied until now to electron-impact ionization of hydrogen is because of the different nature of the asymptotic boundary conditions for half and full collisions—the third important difference between ionization by photon impact and electron impact.

A half collision is subject to complex outgoing-wave boundary conditions, which can be mimicked by complex basis functions. However, a conventional collision is subject to real standing-wave boundary conditions. A standing wave is a real superposition of outgoing- and ingoing-waves, and it cannot be mimicked by complex basis functions, because a complex basis cannot simultaneously account for both outgoing and ingoing waves, only one type or the other. On the other hand, standing waves can be described on a real basis. Therefore the natural basis on which to describe a conventional collision is a real one; but this raises another problem: The response function satisfies outgoing-wave boundary conditions, and outgoing and ingoing waves cannot be distinguished from one another on a real basis!

One way to specify the outgoing-wave character of the response function on a real basis is through the time. In our world, time's arrow points forward, yet time-reversal invariance permits a microscopic system to evolve forward or backward. The physical branch of the response function, or more generally Green's function, is the branch for which time's arrow points forward in *each* (sub)channel. The nonphysical branches are those for which time's arrow points backward in some, perhaps all, (sub)channels. In place of many spatial coordinates, we can specify the physical branch through a single time coordinate. By exploiting its analyticity with respect to its underlying (complex) time scale, the resolvent can be expanded as a series of Laguerre polynomials in the Hamiltonian H. This permits H to be represented on a real basis, and puts half and full collisions on the same footing.

In the next section those details of the method that are relevant to the calculation reported here are sketched. A fuller account is given in [12]. I include some aspects of the method not discussed in [12] in Sec. II. Results for electron-impact ionization of hydrogen are presented in Sec. III, where I also provide an interpretation of these results. The shape of the energy distribution appears to reflect both the competition between escape and recapture, and the substantial post-collision exchange of energy between the electrons.

II. METHOD

A. Flux formulas

Consider a three-body system, with two of the particles bound in the incoming (initial) channel. Let $|\psi_{\rm in}\rangle$ represent the initial unperturbed state of the system, and let P denote a projection operator which projects onto $|\psi_{\rm in}\rangle$ and perhaps other kets that represent unperturbed states in the incoming channel. The orthogonal projection operator is $Q \equiv 1 - P$. We have $P|\psi_{\rm in}\rangle = |\psi_{\rm in}\rangle$ and $Q|\psi_{\rm in}\rangle = 0$. If $H_{\rm in}$ and $W_{\rm in}$ are the unperturbed Hamiltonian and the perturbation, respectively, in the in-channel, the full Hamiltonian is

$$H \equiv H_{\rm in} + W_{\rm in}. \tag{2}$$

However, it is convenient to isolate that part of H, say H_0, which commutes with P, and therefore with Q:

$$H = H_0 + W_0, \tag{3}$$

$$[P, H_0] = 0, \tag{4}$$

where the interaction W_0 vanishes for asymptotically large separations of the particles.

To incorporate some of the (non-Coulombic) distortion of the initial state, we introduce a "static" potential $W_{\rm st}$ which cannot induce transitions out of P space, i.e. $PW_{\rm st}Q = 0$. For example, we could choose $W_{\rm st}$ to be $PW_{\rm in}P$. We represent the incoming distorted wave by $|\psi_{\rm d}^+\rangle$; it is an eigenket of a distorted-wave Hamiltonian $H_{\rm d}$. We can decompose the full Hamiltonian as

$$H = H_{\rm d} + W_{\rm d}, \tag{5}$$

where $W_{\rm d}$ is the distorted-wave perturbation,

$$W_{\rm d} \equiv W_{\rm in} - W_{\rm st}. \tag{6}$$

We assume that $W_{\rm st}$ is sufficiently simple that the equation $H_{\rm d}|\psi_{\rm d}^\pm\rangle = E|\psi_{\rm d}^\pm\rangle$ can be solved "exactly."

By considering the asymptotic flux, it was shown in [12] that the rate Γ_Q for transitions to those states that lie in Q space is

$$\Gamma_Q = 2{\rm Im}\langle\psi_{\rm d}^+|W_{\rm d}G^-(E)QW_0P[1 + G^+(E)W_{\rm d}]|\psi_{\rm d}^+\rangle, \tag{7}$$

where E is the (real) energy of the system, where

$$G^+(E) \equiv 1/(E - H) \tag{8}$$

is the physical branch of the resolvent, and where $G^-(E) = [G^+(E)]^\dagger$. Hence, the rate is a volume integral over the resolvent. The evaluation of the resolvent is addressed below.

To derive an expression for the breakup amplitude for a system composed of three charged particles, we introduce a simple effective Hamiltonian $H_{\rm eff}$ which differs from H by an effective perturbation $W_{\rm eff}$:

$$H = H_{\rm eff} + W_{\rm eff}. \tag{9}$$

We require that $W_{\rm eff}$ vanishes faster than the inverse of each interparticle distance *as the particles move along classical straight-line asymptotes*. Therefore we express $W_{\rm eff}$ as a linear combination of Coulomb potentials whose effective charges are chosen so that $W_{\rm eff}$ vanishes when the particles follow classical straight-line motion. This is a physically reasonable constraint, since three charged particles can reach dynamic equilibrium most efficiently if they shield one another. In the case where one particle is infinitely massive, the effective charges satisfy the well-known condition identified by Peterkop [17,18] and by Rudge and Seaton [19,20]. The distorted-wave form of the breakup amplitude is [12]

$$A = \langle\Psi_{\rm eff}^-|QW_{\rm d}|\psi_{\rm d}^+\rangle + \langle\Psi_{\rm eff}^-|(W_{\rm eff}Q + QW_0P - PW_0Q)G^+(E)W_{\rm d}|\psi_{\rm d}^+\rangle, \tag{10}$$

where $|\Psi_{\rm eff}^\pm\rangle$ is an eigenket of $H_{\rm eff}$.

B. Electron-impact ionization of hydrogen

Let us focus on the electron-impact ionization of hydrogen. The first term on the right side of Eq. (10) is of first order in electron-electron correlation, beyond final-state screening. Electron-electron correlation is fully incorporated through the addition of the second term. Suppose that electron 1 is initially bound in the ground state to an infinitely massive nucleus whose atomic number is $Z = 1$, and that electron 2 is free. Let $\vec{r}_1$ and $\vec{r}_2$ locate the bound and incident electrons, 1 and 2, respectively, at distances r_1 and r_2 from the nucleus; the separation of the electrons is r_{12}. The following expressions must be symmetrized since the electrons are identical. The in-channel first-order perturbation is

$$W_{\rm in}(r_2, r_{12}) = e^2\left(\frac{1}{r_{12}} - \frac{1}{r_2}\right), \tag{11}$$

where $-e$ is the electron charge. We choose the static potential to be the interaction experienced by the incident electron when averaged over the ground-state motion of the bound electron:

$$W_{\rm st}(r) = -\frac{Ze^2}{a_0}\left(1 + \frac{a_0}{Zr}\right)e^{-2Zr/a_0}, \tag{12}$$

where a_0 is the Bohr radius and $Z = 1$. The in-channel distorted-wave perturbation is

$$W_{\rm d}(r_1, r_2, r_{12}) = e^2\left(\frac{1}{r_{12}} - \frac{1}{r_2}\right) + \frac{Ze^2}{a_0}\left(1 + \frac{a_0}{Zr_2}\right)e^{-2Zr_2/a_0}, \tag{13}$$

with $Z = 1$. In contrast to the first-order perturbation, the distorted-wave perturbation is finite at $r_2 = 0$ (leaving aside the exceptional case when r_1 also vanishes). Hence the substantial *virtual* energy transfer which results from elastic scattering from the Coulomb singularity at the nucleus is built into the distorted-wave scattering wave function.

The projection operator Q projects onto the double continuum of the negative hydrogen ion. By using the exact projection operator, we ensure that double escape is not

contaminated by single escape. We have

$$Q = q_1 \otimes q_2, \tag{14}$$

where q projects onto the continuum of the hydrogen atom, with the subscript $i = 1$ or 2 referring to electron 1 or 2. Let $|\vec{k}; Z'; \pm\rangle$ represent a continuum state, normalized on the momentum scale, in which an electron moves in a pure Coulomb potential with strength Z' (not necessarily the same as Z) and with asymptotic momentum that either initially (+) or finally (−) is $\vec{k}$. We have (with $Z = 1$)

$$q = \int d^3\vec{k}\ |\vec{k}; Z; \pm\rangle\langle\vec{k}; Z; \pm|. \tag{15}$$

Note, incidentally, that the product $|\vec{k}_1; Z; \pm\rangle \otimes |\vec{k}_2; Z; \pm\rangle$ does not correctly represent two electrons in the continuum, even at asymptotically large distances, since it does not take into account the long-range electron-electron interaction. Nevertheless, our integral representation of Q, wherein integration is performed over all $\vec{k}_2$ and $\vec{k}_2$, correctly projects onto the entire double continuum; this follows from closure.

In the exit channel, the electrons move quasi-independently; electron i moves in a pure Coulomb potential whose strength is the effective atomic number $Z_i = Z - \Delta_i$ where Δ_1 and Δ_2, respectively, account for the dynamic screening of the nucleus from electron 1 by electron 2, and *vice versa*. Therefore the effective potential in the out-channel is

$$W_{\rm eff}(r_1, r_2, r_{12}) = e^2\left(\frac{1}{r_{12}} - \frac{\Delta_1}{r_1} - \frac{\Delta_2}{r_2}\right). \tag{16}$$

Suppose that electrons 1 and 2 emerge from the collision with energies E_1 and E_2, and with momenta $\vec{k}_1$ and $\vec{k}_2$, respectively. The relative momentum of the electrons is $\vec{k}_{12} = \vec{k}_1 - \vec{k}_2$. The screening parameters are $\Delta_i = (k_i/k_{12})^2(\hat{k}_i \cdot \hat{k}_{ij})$, $j \neq i$ [17–20]. They are independent of both the atomic number of the nucleus and the total energy $E = E_1 + E_2$ of the system, and they can be expressed in terms of the ratio of the speeds and the relative direction of motion of the emergent electrons. Let electron 1 be the slower of the two electrons; the ratio of speeds is

$$\alpha \equiv k_1/k_2, \tag{17}$$

which varies from 0 to 1. In terms of α and the relative direction of motion $(\hat{k}_1 \cdot \hat{k}_2)$, we have

$$\Delta_1 = \frac{1 - (\hat{k}_1 \cdot \hat{k}_2)/\alpha}{[1 - 2(\hat{k}_1 \cdot \hat{k}_2)/\alpha + 1/\alpha^2]^{3/2}}, \tag{18}$$

$$\Delta_2 = \frac{1 - (\hat{k}_1 \cdot \hat{k}_2)\alpha}{[1 - 2(\hat{k}_1 \cdot \hat{k}_2)\alpha + \alpha^2]^{3/2}}. \tag{19}$$

The eigenket $|\Psi^{\pm}_{\rm eff}\rangle$ of the effective Hamiltonian $H_{\rm eff}$ is

$$|\Psi^{\pm}_{\rm eff}\rangle = |\vec{k}_1; Z_1; \pm\rangle \otimes |\vec{k}_2; Z_2; \pm\rangle, \tag{20}$$

which in position space is the 2C wave function. The screening parameters vary significantly as α varies from 0 to 1, and they are sensitive to the relative direction $\hat{k}_1 \cdot \hat{k}_2$ in which the electrons move. While Δ_2 is always positive, Δ_1 can be positive or negative depending on whether α is larger or smaller, respectively, than $\hat{k}_1 \cdot \hat{k}_2$. The slower electron 1 will always partially shield electron 2 from the nucleus, but electron 2, by pushing electron 1 toward the nucleus, can effectively increase the charge of the nucleus experienced by electron 1, which amounts to negative screening.

Let us illustrate two cases: (i) When electron 1 emerges with an infinitesimally small speed, we have $\alpha = 0$, $\Delta_1 = 0$, and $\Delta_2 = 1$, so that $Z_1 = Z$ and $Z_2 = Z - 1$, independently of the relative direction of escape, $\hat{k}_1 \cdot \hat{k}_2$. This expresses the reasonable result that the infinitesimally slow electron 1 experiences the full charge of the nucleus and maximally screens electron 2. (ii) When the two electrons emerge with equal speeds, we have $\alpha = 1$ and $|\Delta_1| = \Delta_2 = 1/[1 - (\hat{k}_1 \cdot \hat{k}_2)]^2$; but Δ_1 can be positive or negative depending on the relative direction of escape. If the electrons emerge back to back, both Δ_1 and Δ_2 are positive, equal to 1/4; but if the electrons emerge in the same direction, Δ_1 is infinitely negative and Δ_2 is infinitely positive. Infinite screening expresses the reasonable result that if the electrons move side by side, they infinitely repel one another; thus the (infinitesimally) slower electron is pushed with infinite force toward the nucleus, while the (infinitesimally) faster electron is pushed with infinite force away from the nucleus.

C. Resolvent

The resolvent has an underlying time scale, t_0 say, which we expose by writing

$$G(E) = -it_0 \int_0^\infty d\tau\ e^{i(t_0E)\tau} U(t_0\tau), \tag{21}$$

where $\tau = t/t_0$ is a dimensionless time and $U(t) \equiv e^{-itH}$ is the time-translation operator (we put $\hbar = 1$). The dichotomy posed by time's arrow is illustrated by the correlation amplitude $C(t) \equiv \langle a|U(t)|a\rangle$, where $|a\rangle$ is any normalizable ket which represents a physically realistic localized wave packet. An informal examination [23] reveals that $C(t)$ has a pair of second-order branch points, one at $t = \infty$ and the other at some finite point in the complex t plane. Although the initial state of a system can be uniquely defined at some finite point in time, the system can evolve either forward or backward. Hence the state at the single point $t = \infty$ is not single-valued; it depends on the direction of evolution to this point. The branch point which is paired with the branch point at infinity is at a distance of the order of t_0 from the origin, and it sets the time scale of the system's evolution.

The time interval over which the evolution of the system can be described adequately is characterized by

$$\mathcal{T}_{\rm max} = 1/(t_0\Delta E), \tag{22}$$

where ΔE is the (positive) separation of the two eigenvalues adjacent to E of the finite-dimensional matrix that in practice represents H. In view of this, we replace the upper limit of the integral on the right side of Eq. (21) by a finite time $\mathcal{T}$ that is of order $\mathcal{T}_{\rm max}$; thus in place of Eq. (21) we have

$$\frac{1 - e^{it_0E\mathcal{T}}U(t_0\mathcal{T})}{E - H} = -it_0 \int_0^{\mathcal{T}} d\tau\ e^{i(t_0E)\tau} U(t_0\tau). \tag{23}$$

Let $|\mathcal{E}\rangle$ be an eigenket of a matrix representation of H, normalized to unit length; the eigenvalue is $\mathcal{E}$. Using closure for the eigenkets of the matrix representation of H, we integrate

over τ to give

$$\frac{1-e^{it_0E\mathcal{T}}U(t_0\mathcal{T})}{E-H}=\sum_{\mathcal{E}}\left(\frac{1-e^{it_0(E-\mathcal{E})\mathcal{T}}}{E-\mathcal{E}}\right)|\mathcal{E}\rangle\langle\mathcal{E}|. \quad (24)$$

If we average over large values of $\mathcal{T}$, the left side of Eq. (24) averages to $G(E)$.

We can express the exact resolvent as the sum

$$G(E)=G_{\rm off}(E)-iG_{\rm on}(E), \quad (25)$$

where, assuming that H is time-reversal invariant,

$$G_{\rm off}(E)={\rm Re}G(E), \quad (26)$$

$$G_{\rm on}(E)=-{\rm Im}G(E), \quad (27)$$

and where $G_{\rm off}(E)$ and $G_{\rm on}(E)$ are orthogonal:

$$G_{\rm off}(E)G_{\rm on}(E)=0. \quad (28)$$

Here $G_{\rm off}(E)$ is the off-energy-shell, i.e., the principal value, part of $G(E)$; while $G_{\rm on}(E)$ is the on-energy-shell, i.e., the energy-conserving, part. The off-shell part of $G(E)$ is the contribution from short times, $\tau<\mathcal{T}_{\rm max}$, while the on-shell part is the contribution from long times, $\tau\sim\mathcal{T}_{\rm max}$; due to their orthogonality, these two parts do not interfere. From Eq. (24) we have, averaging over $\mathcal{T}\sim\mathcal{T}_{\rm max}$,

$$G_{\rm off}(E)=2\left\langle\sum_{\mathcal{E}}\left(\frac{\sin^2\frac{1}{2}t_0(E-\mathcal{E})\mathcal{T}}{E-\mathcal{E}}\right)|\mathcal{E}\rangle\langle\mathcal{E}|\right\rangle_{\rm av}, \quad (29)$$

$$G_{\rm on}(E)=\left\langle\sum_{\mathcal{E}}\left(\frac{\sin t_0(E-\mathcal{E})\mathcal{T}}{E-\mathcal{E}}\right)|\mathcal{E}\rangle\langle\mathcal{E}|\right\rangle_{\rm av}. \quad (30)$$

If $|t_0(E-\mathcal{E})|\gtrsim 1$, the averaged (over $\mathcal{T}$) values of $\sin^2\frac{1}{2}t_0(E-\mathcal{E})\mathcal{T}$ and $\sin t_0(E-\mathcal{E})\mathcal{T}$ are $\frac{1}{2}$ and 0, respectively. Hence those terms in the sums over $\mathcal{E}$ for which $|t_0(E-\mathcal{E})|\gtrsim 1$ contribute to $G(E)$ an amount that is independent of t_0, and is the same as would be obtained using the spectral decomposition of the resolvent. However, the averaged contribution to $G_{\rm off}(E)$ from terms for which $|t_0(E-\mathcal{E})|<1$ is sensitive to t_0 due to cancellation near the singularity at $\mathcal{E}=E$. To put this another way, if $|\Psi\rangle$ represents a realistic wave packet, the averaged contribution to $\langle\Psi|G_{\rm off}(E)|\Psi\rangle$ from terms for which $|t_0(E-\mathcal{E})|<1$ depends on how rapidly $|\langle\mathcal{E}|\Psi\rangle|^2$ varies with $\mathcal{E}$ in the neighborhood of E, and this in turn depends on the value of t_0. On the other hand, the averaged contribution to $G_{\rm on}(E)$ from such terms is insensitive to t_0 since the on-shell part of the resolvent derives its main contribution from times much longer than t_0.

We cannot assign t_0 a unique value since it is a characteristic time. Moreover, to represent the resolvent accurately, we must take account of the branch point of the correlation function at $\sim t_0$. Although we have not built the branch point at infinity into the correlation function, we have at least chosen the correct branch, the "physical" branch, of $G(E)$ by integrating along the positive real time axis. The branch point at $\sim t_0$ can be rendered innocuous by making a conformal transformation which maps each half of the complex t plane onto a unit disk. Thus we divide the t plane into two half planes by the line ${\rm Im}\,t/{\rm Re}\,t=\tan\phi$, where $0<\phi<\pi/2$, and we map each half onto the disk $|u|<1$, where in terms of the dimensionless time τ $(=t/t_0)$,

$$u=\frac{\tau+ie^{i\phi}}{\tau-ie^{i\phi}}. \quad (31)$$

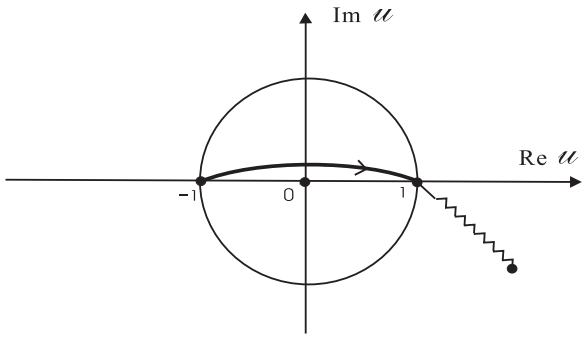

FIG. 1. One-half of the τ plane mapped onto the unit disk $|u|<1$. The physical branch of the resolvent is associated with an integration contour which runs from $u=-1$ to $u=1$ in the upper half of the unit disk. The branch cut (zig-zag line) of the temporal correlation function lies outside the disk.

The transformation from τ to u places the branch point at $\sim t_0$ outside the disk and turns the contour of integration on the right side of Eq. (2) from the line along the real *positive* τ axis to a path from $u=-1$ to $u=1$ in the *upper* half of the disk. See Fig. 1.

It follows from the generating function for the associated Laguerre polynomials $L_n^{(m)}(2z)$ that $U(t)$ has the power-series representation

$$U(t)=e^{-t_\phi H}\left(1-2t_\phi H\sum_{n=1}^{\infty}\frac{1}{n}L_{n-1}^{(1)}(2t_\phi H)u^n\right), \quad (32)$$

where $t_\phi\equiv t_0e^{i\phi}$ is a complex unit of time. This expansion converges for all $|u|<1$. The branch point at $t\sim\infty$ sits at the end of the contour, on the edge of the disk at $u=1$. It is merely a technical nuisance, which causes the integral on the right side of Eq. (23) to fluctuate as $\mathcal{T}$ increases. We obtain a stable result by averaging over large values of $\mathcal{T}$, which smooths out the fluctuations. Inserting the representation of $U(t)$ in powers of u into the right side of Eq. (23), and integrating over τ from 0 to $\mathcal{T}$, yields

$$G(E)=-it_\phi e^{-t_\phi H}\left(\mathcal{I}_0(2Et_\phi,\mathcal{T}_{-\phi})-2t_\phi H\sum_{n=1}^{\infty}\frac{1}{n}\mathcal{I}_n(2Et_\phi,\mathcal{T}_{-\phi})L_{n-1}^{(1)}(2t_\phi H)\right), \quad (33)$$

where $\mathcal{T}_\phi=\mathcal{T}e^{i\phi}$ and where it is understood that the coefficients $\mathcal{I}_n$ are to be averaged over large values of $\mathcal{T}$. These coefficients satisfy simple three-term recurrence relations.

After averaging over $\mathcal{T}$ we obtain the same result for $G_{\rm on}(E)$ whether we use Eq. (33) or (30). One merit of Eq. (33) is that it is not necessary to diagonalize H, and a recurrence relation can be used for $L_{n-1}^{(1)}(2t_\phi H)$. There are several ways of performing the average over $\mathcal{T}$. Previously, the averaging was done explicitly. In the present work, we average implicitly by means of Padé extrapolation [24]. The result is not necessarily more accurate than that obtained by explicit averaging, but it

is certainly more robust. Thus we constructed a sequence by evaluating the right side of Eq. (33) at equally spaced large values of $\mathcal{T}$, and we extrapolated this sequence using Wynn's epsilon algorithm [25].

In the Appendix, we consider how bound states affect the behavior of the temporal correlation amplitude at asymptotically large times. We show that if a two-body system has an infinite number of bound states which accumulate at threshold, they contribute to the decay rate at energies just above threshold through the correlation amplitude. The possible relevance of this to electron-impact ionization of hydrogen is that while the hydrogen negative ion H^- has only one bound state, it has infinitely many doubly excited states that accumulate at the complete-breakup threshold.

D. Formally nonconvergent integrals and the post-prior discrepancy

The second term on the right side of Eq. (10), specifically the part $\langle\Psi^-_{\rm eff}|W_{\rm eff}QG^+(E)W_{\rm d}|\psi^+_{\rm d}\rangle$, is a volume integral that is not formally convergent, since the effective potential $W_{\rm eff}$ falls off with increasing distance only as a sum of Coulomb potentials. However, the integrand oscillates, and the contribution from large distances washes out. Therefore the integral can be assigned a meaningful value in just the same way that the formally nonconvergent integral $\int_0^\infty dr\,\sin kr$ can be assigned the value $1/k$. One way to find the correct "physical" value of $\langle\Psi^-_{\rm eff}|W_{\rm eff}QG^+(E)W_{\rm d}|\psi^+_{\rm d}\rangle$ is by radius-averaging [26,27]. Another way, the one used here, is Padé resummation. The resolvent, or rather the response ket $G^+(E)W_{\rm d}|\psi^+_{\rm d}\rangle$, is expanded on a finite basis, so the integral $\langle\Psi^-_{\rm eff}|W_{\rm eff}QG^+(E)W_{\rm d}|\psi^+_{\rm d}\rangle$ is a finite sum of well-defined terms. A sequence can be formed from the partial sums, and extrapolated by using once again Wynn's epsilon algorithm [25].

In principle we could omit the projection operators in the expression, Eq. (10), for the breakup amplitude, i.e., we could put $P=1$ and $Q=0$. However, the numerical value of the resulting expression is likely to be inaccurate owing to spurious mixing of complete breakup with partial breakup. Nevertheless, let us do this for the purpose of simplifying the following discussion. Thus the first-order term becomes $\langle\Psi^-_{\rm eff}|W_{\rm d}|\psi^+_{\rm d}\rangle$. Recalling that $H_{\rm d}|\psi^+_{\rm d}\rangle = E|\psi^+_{\rm d}\rangle$, and using Eq. (5), we have

$$\langle\Psi^-_{\rm eff}|W_{\rm d}|\psi^+_{\rm d}\rangle = \langle\Psi^-_{\rm eff}|(H-E)|\psi^+_{\rm d}\rangle. \tag{34}$$

If we apply Green's theorem to the last matrix element, we find that the surface term at infinity does not vanish, but it washes out upon radius-averaging so that H is effectively Hermitian. Recalling that $H_{\rm eff}|\Psi^\pm_{\rm eff}\rangle = E|\Psi^\pm_{\rm eff}\rangle$, and using Eq. (9), we have

$$\langle\Psi^-_{\rm eff}|W_{\rm d}|\psi^+_{\rm d}\rangle = \langle\Psi^-_{\rm eff}|W_{\rm eff}|\psi^+_{\rm d}\rangle. \tag{35}$$

Hence, we can use either the prior- or postcollision interaction, $W_{\rm d}$ or $W_{\rm eff}$, in the first-order term. However, while the volume integral on the left side of Eq. (35) is formally convergent, because in position space $W_{\rm d}|\psi^+_{\rm d}\rangle$ falls off as the inverse square of increasing distance, the volume integral on the right side is not, because in position space $W_{\rm eff}|\psi^+_{\rm d}\rangle$ falls off only as the inverse of increasing distance. Therefore, from the numerical standpoint, the "prior form" of the first-order term is expected to be more accurate than the "post form"; this is an example of the "post-prior discrepancy" which is well known from the study of rearrangement collisions.

III. RESULTS

We have applied the method described in the previous section to ^1S-wave electron-impact ionization of hydrogen, and in this section we discuss the results. The Hamiltonian, the response function, and the 2C wave function were represented on a discrete basis composed of real basis functions, each one an appropriately symmetrized product of two real radial Sturmian functions and a bipolar spherical harmonic.

Although the prior form of the first-order term is potentially more accurate, its accuracy is limited in practice by the Coulomb singularity at the point of coalescence of the two electrons, a singularity which produces a cusp that is not built into our basis. In Table I, we show estimates of the post and prior forms of the simplified first-order ionization amplitude—the right and left sides, respectively, of Eq. (35)—for various values of the ratio E_1/E_2 of the energies, and for various values of the relative direction $\hat{k}_1\cdot\hat{k}_2$, of the emergent electrons. These estimates were obtained using a basis which includes only one pair, the pair (0,0), of individual electron angular momenta, and 40 radial Sturmian functions per electron. After expanding the 2C-wave ket $|\Psi^-_{\rm eff}\rangle$ on the basis, the projections of $W_{\rm d}|\psi^+_{\rm d}\rangle$ and $W_{\rm eff}|\psi^+_{\rm d}\rangle$ on each base ket were evaluated to high accuracy using Gauss-Laguerre quadrature. Thereby we expressed the first-order amplitude as a sum of 1600 highly accurate matrix elements. The prior-form sum converges only slowly due to the intrusion of the Coulomb singularity. The results of summing the prior form are shown in the column titled "prior" in Table I; these results are accurate only to the three places given (perhaps only two places where the entries are very small). The columns titled "post (direct)" and "post (Padé)" refer to estimates of the post form of the amplitude obtained by direct summation and by Padé resummation, respectively. Direct summation of the post form is not meaningless, but nor is it very accurate, since the sum represents a formally nonconvergent integral. Padé resummation of the post form markedly improves the accuracy; this is because a Padé approximant can incorporate the poles of a formally nonconvergent integral, such as the simple pole at $k=0$ of $\int_0^\infty dr\,\sin kr$.

All of the remaining results presented in this section were obtained using a basis which includes four pairs (l_1,l_2) of individual electron angular momenta, i.e., $0\leqslant l_1=l_2\leqslant 3$, and either 40 or 50 radial Sturmian functions per electron per angular momentum quantum number. Thus we used a basis whose total size is either 5100 or 7320.

We denote by $d\sigma(E_1,E)/dE_1$ the singly differential cross section for electrons 1 and 2 to emerge with energies E_1 and $E_2=E-E_1$, respectively, where E is the total energy of the system, i.e., the impact energy relative to the breakup threshold. The integrated cross section is

$$\sigma(E) = \int_0^{E/2} dE_1\,\frac{d\sigma(E_1,E)}{dE_1}, \tag{36}$$

and this is shown in Fig. 2 for ^1S-wave electron-impact ionization of hydrogen over a range of impact energies. The cross section was calculated in two different ways, directly

TABLE I. Estimates of the post and prior forms of the simplified first-order amplitude—the right and left sides, respectively, of Eq. (35)—for ^1S-wave electron-impact ionization of hydrogen at an impact energy of 27.2 eV. These estimates were obtained using a basis which includes only one pair, the pair (0,0), of individual electron angular momenta, and 40 radial Sturmian functions per electron. Results are shown for various energy ratios E_1/E_2 and relative directions $\hat{k}_1 \cdot \hat{k}_2$ of emission. The corresponding ratios Z_1/Z_2 of the effective charges are also shown. The headings "post (direct)" and "post (Padé)" refer to estimates of the post form of the amplitude determined by direct summation and Padé resummation, respectively, over the basis. The columns headed "% error" display the relative errors in each of the two post-form estimates as measured against the more accurate prior-form estimate. Numbers in brackets denote powers of 10.

E_1/E_2	$\hat{k}_1 \cdot \hat{k}_2$	Z_1/Z_2	Prior	Post (direct)	% error	Post (Padé)	% error
0	0	∞	9.72[−4]	−1.52[−3]	2.60[2]	9.66[−4]	6.0[−4]
0.14	−1	5.17	2.04[−1]	2.37[−1]	1.60[1]	2.04[−1]	2.3[−1]
0.14	−0.5	6.75	1.89[−1]	2.54[−1]	3.40[1]	1.89[−1]	4.2[−1]
0.14	0	13.9	1.50[−1]	2.83[−1]	8.90[1]	1.49[−1]	5.5[−1]
0.14	0.5	−12.8	3.21[−2]	2.96[−1]	8.20[2]	3.15[−2]	9.1[−1]
0.14	1	−2.29	−7.00[−2]	−1.71[−1]	1.40[2]	−5.37[−2]	2.3[1]
0.33	−1	2.51	2.38[−1]	3.12[−1]	3.10[1]	2.36[−1]	6.5[−1]
0.33	−0.5	2.92	2.30[−1]	3.11[−1]	3.50[1]	2.27[−1]	1.0
0.33	0	4.32	2.01[−1]	2.65[−1]	3.20[1]	1.63[−1]	1.9[1]
0.33	0.5	−20.2	5.34[−2]	−2.73[−2]	1.50[2]	5.31[−2]	1.5[−1]
0.33	1	−1.08	2.42[−4]	2.92[−2]	1.20[4]	4.69[−3]	8.2[2]
0.6	−1	1.53	2.52[−1]	2.43[−1]	3.30	2.51[−1]	2.4[−1]
0.6	−0.5	1.64	2.47[−1]	2.58[−1]	4.20	2.47[−1]	2.6[−1]
0.6	0	1.97	2.31[−1]	3.05[−1]	3.20[1]	2.31[−1]	5.8[−2]
0.6	0.5	5.51	1.30[−1]	3.91[−1]	2.00[2]	1.31[−1]	3.8[−1]
0.6	1	−0.89	2.34[−5]	2.41[−6]	9.00[1]	3.39[−17]	1.0[2]
1	−1	1	2.56[−1]	3.62[−1]	4.10[1]	2.54[−1]	8.4[−1]
1	−0.5	1	2.53[−1]	3.57[−1]	4.10[1]	4.27[−1]	6.9[1]
1	0	1	2.42[−1]	3.09[−1]	2.80[1]	2.62[−1]	8.4
1	0.5	1	1.85[−1]	5.06[−3]	9.70[1]	2.21[−1]	1.9[1]

(circles) from the integrated rate expressed by Eq. (7) above, and indirectly (diamonds) by first calculating the amplitude using Eq. (10) above, squaring it, and integrating over the angles of ejection of both electrons and the energy of one of the electrons. Of course, the two sets of results should agree,

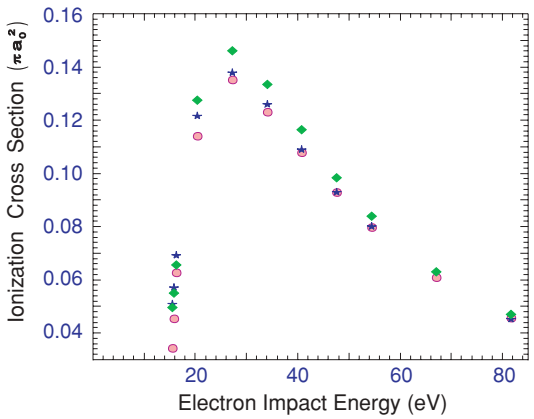

FIG. 2. (Color online) Integrated cross section for ionization of a ground-state hydrogen atom by ^1S-wave electron impact. Stars: data from Bartlett and Stelbovics [7]. Circles: present results, obtained by directly calculating the integrated rate. Diamonds: present results, obtained by calculating the amplitude, which is then squared and integrated over the ejection angles of both electrons and the energy of one of the electrons. All three sets of data have the same abscissa, except at 67 eV where no data from [7] is available.

but they do not—more on that in a moment. We also show the results (stars) of Bartlett and Stelbovics [7]. The results we obtained indirectly from the amplitude (diamonds) agree fairly well with the results of Bartlett and Stelbovics at low (below 16 eV) and high (above 60 eV) energies, but not at intermediate energies. On the other hand, the results we obtained directly from the rate (circles) agree well with the results of Bartlett and Stelbovics at impact energies at 27 eV and above. Below 27 eV, our results (those obtained directly from the rate) fall too rapidly as the energy approaches threshold—they are not converged with respect to the number of radial basis functions, because the distance over which breakup occurs increases without limit as the energy approaches threshold. In principle this deficiency could be remedied by including a larger number of radial basis functions.

On the other hand, the origin of the discrepancies between the results we calculated directly from the rate (circles) and those we calculated indirectly from the amplitude (diamonds) is more subtle. At impact energies of more than about 27 eV, where $\sigma(E)$ has its maximum, both sets of results are reasonably well converged with respect to the number of radial basis functions; yet although the discrepancies steadily diminish as the impact energy increases beyond about 27 eV, they remain evident even at 80 eV. The reason for the persistent disagreement is a lack of convergence with respect to the number of pairs of individual electron angular momenta. As each electron moves away from the nucleus, its angular momentum about the nucleus diverges logarithmically, since each electron exerts a long-range Coulomb torque on the

other [10,11]. (Note, however, that the net torque $\vec{r}_1 \times \vec{F}_{21} + \vec{r}_2 \times \vec{F}_{12}$ vanishes, since the force $\vec{F}_{21}$ exerted by electron 2 on electron 1 is equal and opposite to the force $\vec{F}_{12}$ exerted by electron 1 on electron 2, and since $\vec{r}_1 - \vec{r}_2$ is parallel to $\vec{F}_{21}$. Therefore the total angular momentum of the electrons about the nucleus does not change.) It is questionable whether either the rate or the amplitude truly converge with respect to pairs of individual electron angular momenta, since the inclusion of more angular momenta in the basis would necessitate inclusion of more radial basis functions, and in turn the Coulomb torque would act over a larger volume, so still more individual angular momenta would have to be added, and so on. Nevertheless, it is likely that an expansion in angular momentum pairs exhibits *pseudo*convergence because the *effective* reaction volume over which breakup takes place is finite, so the *effective* torque remains finite. Just as an asymptotic series can yield accurate results even though it does not converge, it is possible that accurate estimates of the amplitude and rate can be obtained by including a limited number of pairs of angular momenta [28]. This is all the more likely because the rotational energy of each electron only barely grows with distance, and asymptotically approaches a constant. Moreover, the characteristic linear dimension of the effective reaction volume decreases as the impact energy increases, and this is reflected in Fig. 2 by the steady improvement, as the impact energy rises above 27 eV, in agreement between the results we derived from the rate and those we derived from the amplitude.

Since the amplitude contains specific information about the final state, whereas the rate does not, one might wonder whether our results for $\sigma(E)$ derived from the amplitude are more accurate than those derived from the rate, in spite of the good agreement, above 20 eV, between our results derived from the rate and the results of Bartlett and Stelbovics. We cannot provide much insight at present. The amplitude, because it contains more information than the rate, is more sensitive than the rate to the dynamics at large distances, and hence it is more sensitive to the number of pairs of individual electron angular momenta included in the basis. On the other hand, our results for $\sigma(E)$ derived from the rate *seem* to be converged with respect to the number of angular momenta pairs—but this may be illusory because the growth in angular momenta with distance is slow, i.e., logarithmic. The lack of convergence with respect to angular momenta pairs is more obvious for the amplitude because we have not treated angular momentum in the same way in the final state as in the basis: Our approximate 2C final-state wave function implicitly accounts for an indefinite exchange of angular momenta between the electrons through effective charges that depend on the individual linear momenta of the electrons, but this cannot be realized because we have restricted the number of angular momenta pairs in our basis. Clearly, further investigation into the role played by the Coulomb torque is needed, and will be undertaken in the future.

However, the Coulomb torque does not play a significant role at energies very close to threshold, for in this energy region, the repulsion of the electrons ensures that the dominant configuration in the final state is one where the electrons escape back-to-back, so the force exerted by one electron on the other is along the line of motion of each electron, and therefore the torque on each electron vanishes [11].

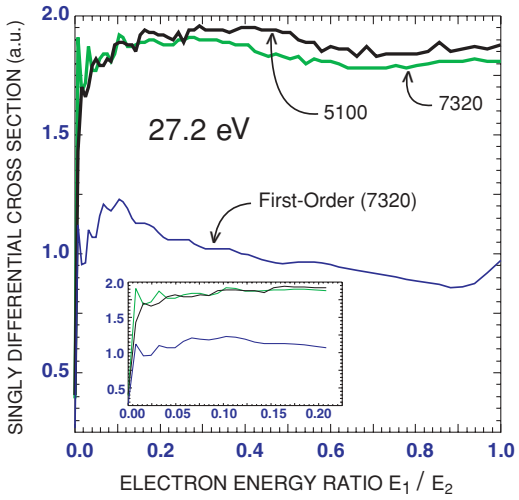

FIG. 3. (Color online) Energy partitioning of the electrons vs the ratio of the electron energies following ionization of ground-state hydrogen by ^1S-wave electron impact at 27.21138 eV. The distribution is symmetric under the interchange of the energies E_1 and E_2 of the electrons, so we do not show it for $0 \leqslant E_2/E_1 \leqslant 1$. Upper lines: Nonperturbative results, basis sizes 5100 and 7320. Lower line: First-order results, basis size 7320. Here "first-order" means that electron correlation, beyond final-state screening, is included only through first order; see Eq. (10) of the text.

Hence consideration of the Coulomb torque does not call into question the Wannier threshold law [1,18,29]. The diminishing importance of the Coulomb torque near threshold is reflected in Fig. 2, where we see that as the energy approaches threshold the agreement between our results for $\sigma(E)$ derived from the amplitude (diamonds) and the results (stars) of Bartlett and Stelbovics improves significantly. As remarked already, our results derived from the rate (circles) deteriorate as the energy approaches threshold due to an insufficient number of radial basis functions in our basis. Though not shown, our results derived from the amplitude also deteriorate, for the same reason, but not as severely and not until the energy is within 2 eV of threshold.

We calculated the singly differential cross section $d\sigma(E_1, E)/dE_1$ by squaring the amplitude given by Eq. (10) and integrating over the angles of ejection of both electrons. In Fig. 3, we show $d\sigma(E_1, E)/dE_1$ vs the ratio E_1/E_2 of the energy of electrons for the case where the impact energy is 27.2 eV, exactly double the energy needed to liberate the bound electron. The differential cross section, which is invariant under the interchange of E_1 and E_2, reveals how the total energy ($E = 13.6$ eV) of the system is partitioned between the electrons. As the ratio E_1/E_2 increases from zero, $d\sigma(E_1, E)/dE_1$ at first rises sharply, accompanied by undulations, but eventually flattens out into a rough (bumpy) plateau; we can understand the main features as follows:

Ionization occurs through a hard collision between the electrons. We suppose that the incident electron (electron 2) emerges from the collision as the faster electron, since this entails the least momentum transfer. The bound electron (electron 1) is not immediately liberated because it takes time for its wave packet to develop into a free-particle wave packet. Let $\mathcal{E}_1$ and $\mathcal{E}_2$ be the electron energies immediately after the

collision. The time it takes electron 1 to travel a distance equal to its de Broglie wavelength after the collision is $\sim\hbar/\mathcal{E}_1$; this is the characteristic time required for the free-particle wave packet to develop. (We have reinstated $\hbar$ so as to make the dimensions clear.) During this time, electron 2, whose speed is $v_2 = \sqrt{2\mathcal{E}_2/\mu}$ where μ is the electron mass, moves a classical distance of order $\hbar v_2/\mathcal{E}_1$, a distance much larger than this electron's de Broglie wavelength $\hbar/(\mu v_2)$ if $\mathcal{E}_2 \gg \mathcal{E}_1$. At this point, the Coulomb interaction energy between the electrons is of order $e^2\mathcal{E}_1/(\hbar v_2)$. This is the energy which is now available to be shared between the electrons as they continue to escape. If it is comparable to (or greater than) $\mathcal{E}_2$, it is likely that over time the electrons will trade energy back and forth so that eventually their energies are distributed uniformly. Hence we expect the energy distribution to be roughly flat in the region where the final electron energies E_1 and E_2 satisfy the criterion introduced in the Introduction, i.e., $E_1/E_2 \gtrsim \sqrt{E_2/(1\ \mathrm{Ry})}$. If this inequality is not satisfied, the amount of energy that can be exchanged postcollision is small, and therefore most of the energy needed to liberate the bound electron must be absorbed abruptly during the collision. In this case, ionization occurs by shakeoff, so we can treat the electrons independently and evaluate the probability amplitude for the bound electron to undergo a transition to the continuum by using the "sudden" approximation of perturbation theory. The amplitude is proportional to the overlap of the bound-state wave function and a continuum-state wave function which describes an electron slowly departing from a nucleus that is dynamically screened by the fast electron. However, if $\mathcal{E}_1 = 0$, the fast electron does not screen the nucleus, and the bound- and continuum-state wave functions are orthogonal. In other words, the probability for shakeoff vanishes at $\mathcal{E}_1 = 0$. Of course, this description is only approximate, so $d\sigma(E_1, E)/dE_1$ is not exactly zero at $E_1 = 0$, but it is small. Furthermore, $d\sigma(E_1, E)/dE_1$ rises sharply as E_1 increases from zero, since the screening parameter Δ_1 comes into play, so the bound- and continuum-state wave functions are no longer orthogonal. As E_1 increases, the postcollision exchange of energy becomes more substantial. In the region $0 \ll E_1/E_2 \ll \sqrt{E_2/(1\ \mathrm{Ry})}$, where electron 1 moves slowly but postcollision energy exchange is non-negligible, electron 1 may give up some of its energy to electron 2 and fall back into a bound state. We presume that this competition between escape and recapture, a competition in which the dynamic screening of the nucleus plays an important role, is reflected by the prominent undulations which appear in the energy distribution in the region of asymmetric energy sharing. These undulations become less prominent as energy sharing becomes more symmetric, where the distribution flattens into a rough plateau.

Putting $E_1 = E_2 = E/2$ in Eq. (1) leads us to expect the energy distribution to be flat in the region near the point of equal-energy-sharing if $E \lesssim 2$ Ry. (This corresponds to an impact energy smaller than 41 eV.) This is consistent with Fig. 3, where $E = 1$ Ry (13.6 eV). The farther below 2 Ry is E, the lower the value of E_1/E_2 for which Eq. (1) can be satisfied, and therefore the wider the range of E_1/E_2 over which the energy distribution is expected to be flat. Energy distributions at two other impact energies, 16.3 and 40.8 eV, are shown in Figs. 4 and 5. Once again, as E_1 increases from zero, $d\sigma(E_1, E)/dE_1$ rises, accompanied by undulations. If we compare Fig. 3, where $E = 13.6$ eV, with Fig. 4, where $E = 2.7$ eV, we see that $d\sigma(E_1, E)/dE_1$ rises less sharply when $E = 2.7$ eV, while its undulations are more numerous. When $E = 2.7$ eV, postcollision energy exchange is more important, and the energy distribution begins to flatten out at lower values of E_1/E_2, while escape vs recapture of the slow electron is more delicate. Note that the energy distributions at both $E = 2.7$ and $E = 13.6$ eV are primarily convex. On the other hand, if we compare Fig. 3, where $E = 13.6$ eV, with Fig. 5, where $E = 27.2$ eV, we see that $d\sigma(E_1, E)/dE_1$ rises more sharply when $E = 27.2$ eV, it subsequently falls, and its undulations do not appear until it begins to fall. When $E = 27.2$ eV, postcollision energy exchange is much less important, and the energy distribution is flat only close to the point of equal energy sharing. These observations conform with Eq. (1).

We remarked above that the long-range Coulomb torque is less important at energies E close to threshold. It is also

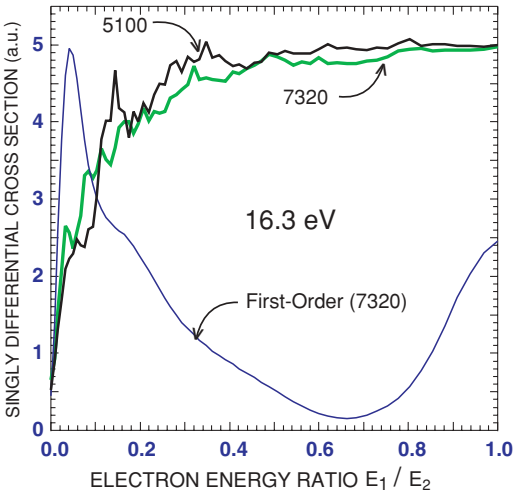

FIG. 4. (Color online) Same as Fig. 3, but for an impact energy of 16.32683 eV.

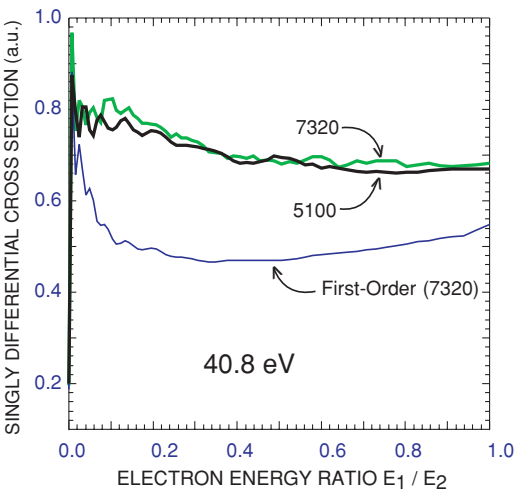

FIG. 5. (Color online) Same as Fig. 3, but for an impact energy of 40.81708 eV.

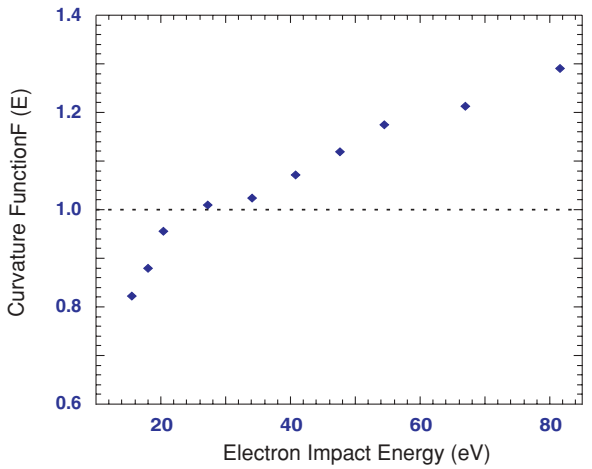

FIG. 6. (Color online) Curvature of the energy distribution of the electrons following ionization of ground-state hydrogen by ^1S-wave electron impact at various energies. The energy distribution is primarily flat, concave, or convex according to whether $F(E) = 1$, $F(E) > 1$, or $F(E) < 1$, respectively.

less important when E_1/E_2 is small, because when the fast electron (electron 2) is far from the nucleus, the slow electron is relatively close, so the position vector $\vec{r}_2$ is nearly parallel to $\vec{r}_2 - \vec{r}_1$, which is parallel to $\vec{F}_{21}$, and hence the Coulomb torque exerted by each electron on the other at large times is small. Therefore, in the region of highly asymmetric energy sharing, we do not expect the energy distribution to be sensitive to the number of pairs of individual electron angular momenta in the basis. We cannot say the same for the plateau region where energy sharing is more symmetric; but we note again that the rotational energy of each electron grows only weakly with distance and is bounded. Although we have not demonstrated convergence of our results—neither with respect to the number of radial functions nor the number of angular momentum pairs in our basis—the prominent features seen in Figs. 3–5, i.e., the sharp rise and undulations of the differential cross section at small values of E_1/E_2, and the plateau at larger values of E_1/E_2, are fairly robust. On the other hand, the small bumps in the plateau region are less robust when the basis size is changed, and we do not know if they have a physical origin.

A simple but crude measure of the curvature of the energy distribution is given by the function $F(E)$ defined by [13]

$$\sigma(E) \equiv \left(\frac{E}{2}\right) F(E) \frac{d\sigma(E_1, E)}{dE_1}\bigg|_{E_1=\frac{E}{2}}. \tag{37}$$

The energy distribution is primarily flat, concave, or convex according to whether $F(E) = 1$, $F(E) > 1$, or $F(E) < 1$, respectively. We show $F(E)$ in Fig. 6; evidently the energy distribution is primarily convex or flat up to 20 eV above the breakup threshold.

We conclude by commenting on a quite dramatic feature of the energy distribution found by Bouri *et al.* [15] in their study of double photoionization of helium at a photon energy of $E = 0.1$ eV above threshold. They found (see their Fig. 2) that the curvature is mostly positive but that it turns sharply negative for $E_1 < 0.06E$. When $E_1 \ll E_2$, we can put $E_2 \approx E$ in our Eq. (1), which implies that if $E = 0.1$ eV, postcollision energy exchange is substantial only when $E_1 > 0.09E$. Thus we interpret the sharp turn in the energy distribution, from positive to negative curvature, to be due to the absence of significant postcollision energy exchange when $E_1 < 0.09E$.

ACKNOWLEDGMENTS

I thank Bernard Piraux for his comments and for providing me with the matrix elements of $1/r_{12}$ used in the calculations described above.

APPENDIX: DISCRETE EIGENSTATES AND DECAY NEAR THRESHOLD

In this Appendix, we examine the influence of bound states on the behavior of the temporal correlation amplitude at asymptotically large times. We consider a two-body system and show that if this system has an infinite number of bound states which accumulate at threshold they do play a role at large times, and through the correlation amplitude they contribute to the decay rate at energies just above threshold.

Consider a single particle of mass μ which moves in a central potential V governed by a Hamiltonian H. Suppose that the particle is prepared in an eigenstate of H represented by $|\psi\rangle$, and that subsequently the particle is perturbed by a short-range interaction W. If the final energy E_K of the particle lies in the continuum, the rate for transitions out of the initial state is

$$\Gamma = -2\,\mathrm{Im}\langle\Psi|G^+(E)|\Psi\rangle, \tag{A1}$$

$$= 2\pi\langle\Psi|\delta(H - E)|\Psi\rangle, \tag{A2}$$

where the normalizable ket $|\Psi\rangle \equiv W|\psi\rangle$ represents the coupling of the perturbation to the initial state. We derive the threshold law for the decay rate in two different ways, first by using Eq. (A2) and then by using the temporal correlation function.

Let $|\Phi_{\vec{k}}\rangle$ be a continuum eigenket of H with eigenvalue $E_k = k^2/(2\mu) + \Delta$, where Δ is a positive shift in the threshold of the continuous spectrum, sufficiently large to ensure that H is positive definite. We normalize $|\Phi_{\vec{k}}\rangle$ on the momentum scale, so the density of states per energy interval dE is $\mu k d^2\hat{k}$. Writing $\Psi(\vec{k}) \equiv \langle\Phi_{\vec{k}}|\Psi\rangle$ and $\vec{K} \equiv K\hat{k}$, it follows from Eq. (A2) that

$$\Gamma = 2\pi\mu K \int d^2\hat{k}|\Psi(\vec{K})|^2. \tag{A3}$$

If V is a short-range potential, i.e., one which vanishes faster than a Coulomb potential at large distances, the limit of $\Psi(\vec{K})$ as $K \to 0$ exists, and we arrive at the threshold law

$$\Gamma = 8\pi^2\mu K|\Psi(\vec{0})|^2, \quad K \sim 0. \tag{A4}$$

We have assumed that the particle's angular momentum quantum number l is zero. The generalization to nonzero l is straightforward; we need only factor out the k^l dependence from $\Psi(\vec{k})$ before letting $k \to 0$. If V is a long-range potential with an attractive Coulomb tail $-Ze^2/r$, we must extract the

Coulomb distortion factor before letting $k \to 0$. Thus, writing $\Psi(\vec{k}) = 2\pi(Z/a_0 k)\tilde{\Psi}(\vec{k})$, we arrive at the threshold law when V is long range:

$$\Gamma = 16\pi^3 Z(\mu/a_0)|\tilde{\Psi}(\vec{0})|^2, \quad K \sim 0. \tag{A5}$$

Note that the bound-state eigenkets of H played no role in our derivation of the threshold laws; they do not directly contribute to the decay rate through the resolvent.

Using Eq. (21), we can rewrite Eq. (A1) as

$$\Gamma = 2\mathrm{Re}\int_0^\infty dt\; e^{iE_K t} C(t), \tag{A6}$$

where $C(t)$ is the correlation function

$$C(t) = \langle\Psi|e^{-iHt}|\Psi\rangle. \tag{A7}$$

Let us expand $|\Psi\rangle$ on the complete set of eigenkets of H. We denote a bound-state eigenket with eigenvalue E_{bd} by $|\Phi_{E_{\mathrm{bd}}}\rangle$. Writing $\Psi_{E_{\mathrm{bd}}} = \langle\Phi_{E_{\mathrm{bd}}}|\Psi\rangle$, and $C(t) = C_{\mathrm{bd}}(t) + C_{\mathrm{ct}}(t)$, where $C_{\mathrm{bd}}(t)$ and $C_{\mathrm{ct}}(t)$ are the contributions to $C(t)$ from the bound states and the continuum, we have

$$C_{\mathrm{bd}}(t) = \sum_{E_{\mathrm{bd}}} |\Psi_{E_{\mathrm{bd}}}|^2 e^{-iE_{\mathrm{bd}}t}, \tag{A8}$$

$$C_{\mathrm{ct}}(t) = \int d^3\vec{k}\,|\Psi(\vec{k})|^2 e^{-iE_k t}. \tag{A9}$$

Now we let t approach infinity along a ray slightly rotated below the positive real t axis. Each term in the sum over bound states diminishes exponentially (note that $E_{\mathrm{bd}} > 0$ since H is positive-definite). Hence $C_{\mathrm{bd}}(t)$ is negligible. The main contribution to the integral over $\vec{k}$ comes from the region $|k^2 t/\mu| \ll 1$. Changing variables from $\vec{k}$ to $\vec{k}/\sqrt{t}$, and approximating $|\Psi(\vec{k})|^2$ by $|\Psi(\vec{0})|^2$, assuming that V is short range, gives an integral over a Gaussian function which can be evaluated exactly. Hence, neglecting the contribution from the bound states, we have

$$C(t) \approx e^{-i3\pi/4}|\Psi(\vec{0})|^2\left(\frac{2\pi\mu}{t}\right)^{3/2}, \quad t \sim \infty. \tag{A10}$$

Thus $C(t)$ has the asymptotic t dependence which reflects wave-packet spreading. As above, if the particle has nonzero angular momentum l, we should factor out k^l from $\Psi(\vec{k})$ before changing variables. In the limit $K \to 0$, only the region of asymptotically large t contributes to the integral on the right side of Eq. (A6), so we obtain

$$\Gamma = 2\mathrm{Re}\int_0^\infty dt\;\frac{e^{iE_K t}}{t^{3/2}}, \quad K \sim 0. \tag{A11}$$

Integrating over t yields the same threshold law given by Eq. (A4). If V is long range, we must extract from $\Psi(\vec{k})$ the Coulomb distortion factor before letting $k \to 0$. Thus, with $\tilde{\Psi}(\vec{k})$ defined above,

$$C_{\mathrm{ct}}(t) \approx e^{-i\pi/2} 8\pi^2 Z\mu|\tilde{\Psi}(\vec{0})|^2\left(\frac{1}{a_0 t}\right), \quad t \sim \infty \;\; (Z > 0). \tag{A12}$$

Hence in the threshold limit $K \to 0$, the contribution to the rate from the continuum states is

$$16\pi^2 Z\mu|\tilde{\Psi}(\vec{0})|^2\mathrm{Re}\left(\frac{e^{-i\pi/2}}{a_0}\int_0^\infty dt\;\frac{e^{iE_K t}}{t}\right)$$
$$= 8\pi^3 Z(\mu/a_0)|\tilde{\Psi}(\vec{0})|^2, \tag{A13}$$

which is *half* the result given by Eq. (A5). The discrepancy is due to the neglect of $C_{\mathrm{bd}}(t)$. When the potential has an attractive Coulomb tail, an infinite number of bound states accumulate at threshold, and the sum over the bound states on the right side of Eq. (A8) does not converge uniformly in t, so the sum and limit cannot be interchanged. Thus $C_{\mathrm{bd}}(t)$ contributes equally with $C_{\mathrm{ct}}(t)$ to the decay rate at threshold.

[1] A. R. P. Rau, Comments At. Mol. Phys. **14**, 285 (1984).

[2] I. Vinkalns and M. Gailitis, in *Proceedings of the 5th International Conference on Physics of Electronic and Atomic Collisions* (Nauka, Leningrad, 1967), p. 648.

[3] F. H. Read, J. Phys. B **17**, 3965 (1984).

[4] P. Hammond, F. H. Read, S. Cvejanovic, and G. C. King, J. Phys. B **18**, L141 (1985).

[5] M. Gailitis, J. Phys. B **19**, L697 (1986).

[6] J. M. Rost, Phys. Rev. Lett. **72**, 1998 (1994).

[7] P. L. Bartlett and A. T. Stelbovics, Phys. Rev. Lett. **93**, 233201 (2004).

[8] M. Baertschy, T. N. Rescigno, W. A. Isaacs, X. Li, and C. W. McCurdy, Phys. Rev. A **63**, 022712 (2001).

[9] F. H. Read (private communication).

[10] Yu. V. Popov and J. J. Benayoun, J. Phys. B **14**, 3513 (1981).

[11] M. Gailitis, J. Phys. B **23**, 85 (1990).

[12] R. Shakeshaft, Phys. Rev. A **80**, 012708 (2009).

[13] D. Proulx and R. Shakeshaft, Phys. Rev. A **48**, R875 (1993); M. Pont and R. Shakeshaft, J. Phys. B **28**, L571 (1995).

[14] E. Foumouo, Ph. Antoine, B. Piraux, L. Malegat, H. Bachau, and R. Shakeshaft, J. Phys. B **41**, 051001 (2008).

[15] C. Bouri, P. Selles, L. Malegat, and M. G. Kwato Njock, Phys. Rev. A **73**, 022724 (2006).

[16] A. M. Mukhamedzhanov and M. Lieber, Phys. Rev. A **54**, 3078 (1996).

[17] R. K. Peterkop, Opt. Spektrosk. **13**, 153 (1962).

[18] R. K. Peterkop and L. L. Rabik, Theor. Math. Phys. **31**, 502 (1977).

[19] M. R. H. Rudge and M. J. Seaton, Proc. R. Soc. London Ser. A **283**, 262 (1965).

[20] M. R. H. Rudge, Rev. Mod. Phys. **40**, 564 (1968).

[21] Another well-known approximate wave function which describes the asymptotic motion of the two electrons is the 3C wave function, which is a product of three Coulomb wave functions containing static rather than dynamic charges. See M. Brauner, J. S. Briggs, and H. Klar, J. Phys. B **22**, 2265 (1989).

[22] To see how the argument goes, consider potential scattering. Suppose a particle of mass μ is incident with momentum $\hbar\vec{k}$ on a short-range potential V. The amplitude to scatter into the direction $\hat{k}'$ is $f(\vec{k} \to \vec{k}\prime) = -(2\pi/\hbar)^2\mu\langle\Psi^-_{\vec{k}\prime}|V|\vec{k}\rangle$. Write $\langle\Psi^-_{\vec{k}\prime}|V|\vec{k}\rangle = \langle\Psi^-_{\vec{k}\prime}|(E +$

$i0 - H)G^+(E)V|\vec{k}\rangle = \langle\Psi^-_{\vec{k}'}|(H^\dagger - H)G^+(E)V|\vec{k}\rangle$ using $(E - i0 - H)|\Psi^-_{\vec{k}'}\rangle = 0$. Now use Green's theorem to express $f(\vec{k} \to \vec{k}')$ as a surface-integral over the two angles of $\hat{r}$. On the surface, $\langle\vec{r}|G^+(E)V|\vec{k}\rangle \to (2\pi)^{-3/2} f(\vec{k} \to k\hat{r})e^{ikr}/r$ and $\langle\vec{r}|\Psi^-_{\vec{k}'}\rangle \to (2\pi)^{-3/2}[e^{i\vec{k}\prime\cdot\vec{r}} + f(\vec{k}\prime \to k\hat{r})e^{-ikr}/r]$. The surface has area $4\pi r^2$. The surface integral contains a term that is linear in f and another term that is bilinear. The bilinear term falls off as $1/r^2$ and oscillates as e^{2ikr} so it washes out upon radius-averaging. Hence we can replace $|\Psi^-_{\vec{k}'}\rangle$ by $|\vec{k}'\rangle$, to give $f(\vec{k} \to \vec{k}') = -i(1/4\pi)kr \int d^2\hat{r}(1 + \hat{k}' \cdot \hat{r}) f(\vec{k} \to k\hat{r})e^{ikr - i\vec{k}'\cdot\vec{r}}$. Now write $d^2\hat{r} = -2\pi d(\hat{k}' \cdot \hat{r})$ and integrate by parts over $\hat{k}' \cdot \hat{r}$; only the direction $\hat{r} = \hat{k}'$ contributes to the surface integral when $r \sim \infty$, and it reduces to $f(\vec{k} \to \vec{k}')$. It follows that we can replace $\langle\vec{r}|\Psi^-_{\vec{k}'}\rangle$ in $\langle\Psi^-_{\vec{k}'}|(H^\dagger - H)G^+(E)V|\vec{k}\rangle$ by a wave function whose only constraint is that it behaves as $e^{i\vec{k}'\cdot\vec{r}}$ for $\hat{r}$ in the neighborhood of $\hat{k}'$ when $r \sim \infty$. Upon such replacement, the surface integral can be returned to a volume integral. Incidentally, the same idea was used to derive a partial nonperturbative rate for multiphoton transitions; see the Appendix of R. M. Potvliege and R. Shakeshaft, Phys. Rev. A **38**, 6190 (1988).

[23] R. Shakeshaft and B. Piraux, Adv. Theor. Math. Phys. **4**, 1093 (2000).

[24] C. M. Bender and S. A. Orszag, *Advanced Mathematical Methods for Scientists and Engineers* (McGraw-Hill, New York, 1978).

[25] E. J. Weniger, Comput. Phys. Rep. **10**, 189 (1989).

[26] M. Lieber, L. Rosenberg, and L. Spruch, Phys. Rev. D **5**, 1330 (1972); **5** 1347 (1972).

[27] L. Rosenberg, Phys. Scr. **77**, 015305 (2008).

[28] Convergence, or rather pseudoconvergence, was found for the simpler problem of one-photon impact ionization of helium; see Ref. [14].

[29] G. H. Wannier, Phys. Rev. **90**, 817 (1953).